




# Evaluation of the ‘ring sign’ and the ‘core sign’ as a magnetic resonance imaging marker of disease activity and progression in clinically isolated syndrome and early multiple sclerosis

*Multiple Sclerosis Journal—  
Experimental, Translational  
and Clinical*

January–March 2020, 1–11

DOI: 10.1177/  
2055217320915480© The Author(s), 2020.  
Article reuse guidelines:  
sagepub.com/journals-  
permissions

Nelly Blindenbacher\*, Eveline Brunner\* , Susanna Asseyer , Michael Scheel, Nadja Siebert, Ludwig Rasche, Judith Bellmann-Strobl, Alexander Brandt , Klemens Ruprecht, Dominik Meier, Jens Wuerfel\*, Friedemann Paul\* and Tim Sinnecker\*

## Abstract

**Background:** Brain lesions with a hypointense ring or core were described in multiple sclerosis on susceptibility weighted imaging.

**Objective:** The purpose of this study was to study the evolution and prognostic relevance of susceptibility weighted imaging hypointense lesions in clinically isolated syndrome and early multiple sclerosis.

**Methods:** Sixty-six early multiple sclerosis and clinically isolated syndrome patients were followed over a median period of 2.9 years (range 1.6–4.6 years) and underwent 3T magnetic resonance imaging including 3D susceptibility weighted imaging and T2-weighted fluid-attenuated inversion recovery. We assessed the presence of susceptibility weighted imaging hypointense core or ring lesions, and Expanded Disability Status Scale at baseline and follow-up.

**Results:** Of 611 lesions at baseline, 64 (10.5%) had a susceptibility weighted imaging hypointense core, and 28 (4.6%) had a susceptibility weighted imaging hypointense ring. Hypointense ring lesions were larger ( $p < 0.001$ ) and more T1w hypointense ( $p = 0.002$ ) than others. During follow-up, hypointense core lesions became susceptibility weighted imaging isointense (52 lesions, 81%); few developed into hypointense ring lesions (two lesions, 3%). Hypointense ring lesions did not shrink on T2-weighted fluid-attenuated inversion recovery images ( $p = 0.077$ , trend towards more enlargement compared to others), while hypointense core lesions more often shrunk in comparison to lesions without a hypointense core ( $p = 0.002$ ). The number of susceptibility weighted imaging hypointense ring lesions at baseline correlated with Expanded Disability Status Scale progression at follow-up ( $p = 0.021$ ,  $R = 0.289$ ).

**Conclusion:** In our cohort of patients with clinically isolated syndrome or early multiple sclerosis, susceptibility weighted imaging hypointense ring lesions were only rarely detectable, but did not shrink and were associated with future disability progression.

**Keywords:** Multiple sclerosis, clinically isolated syndrome, 3 Tesla MRI, ring sign, susceptibility weighted imaging

Date received: 30 November 2019; accepted: 21 February 2020

## Introduction

Multiple sclerosis (MS) is an inflammatory, demyelinating and neurodegenerative central nervous system disease with distinct brain lesions detectable by magnetic resonance imaging (MRI).<sup>1,2</sup> Recent

studies have identified different MS lesion types based on their paramagnetic properties on gradient echo MRI sequences such as susceptibility weighted imaging (SWI).<sup>3–5</sup> Most importantly, lesions with a SWI hypointense core (‘core sign’), and

\*Equally contributing first and senior authors.

Correspondence to:  
**Friedemann Paul**,  
NeuroCure Clinical Research  
Center, Charité-  
Universitätsmedizin Berlin,  
Charitéplatz 1, 10117 Berlin,



Germany.  
friedemann.paul@charite.de

**Nelly Blindenbacher\***,  
qbig, Department of  
Biomedical Engineering,  
University of Basel,  
Switzerland

**Eveline Brunner\***,  
qbig, Department of  
Biomedical Engineering,  
University of Basel,  
Switzerland

**Susanna Asseyer**,  
Neurocare Clinical Research  
Center, Charité-  
Universitätsmedizin Berlin,  
Germany  
Experimental and Clinical  
Research Center, Charité –  
Universitätsmedizin Berlin,  
and Berlin Institute of Health  
and Max Delbrück Center for  
Molecular Medicine,  
Germany

**Michael Scheel**,  
Neurocare Clinical Research  
Center, Charité-  
Universitätsmedizin Berlin,  
Germany

**Nadja Siebert**,  
Neurocare Clinical Research  
Center, Charité-  
Universitätsmedizin Berlin,  
Germany  
Experimental and Clinical  
Research Center, Charité –  
Universitätsmedizin Berlin,  
and Berlin Institute of Health  
and Max Delbrück Center for  
Molecular Medicine,  
Germany

**Ludwig Rasche**,  
Neurocare Clinical Research  
Center, Charité-  
Universitätsmedizin Berlin,  
Germany  
Experimental and Clinical  
Research Center, Charité –  
Universitätsmedizin Berlin,  
and Berlin Institute of Health  
and Max Delbrück Center for  
Molecular Medicine,  
Germany

**Judith Bellmann-Strobl**,  
Neurocare Clinical Research  
Center, Charité-  
Universitätsmedizin Berlin,  
Germany  
Experimental and Clinical  
Research Center, Charité –  
Universitätsmedizin Berlin,  
and Berlin Institute of Health  
and Max Delbrück Center for  
Molecular Medicine,  
Germany

**Alexander Brandt**,  
Neurocare Clinical Research  
Center, Charité-  
Universitätsmedizin Berlin,  
Germany  
Experimental and Clinical  
Research Center, Charité –  
Universitätsmedizin Berlin,  
and Berlin Institute of Health  
and Max Delbrück Center for

lesions with a SWI hypointense ring ('ring sign') were described.<sup>3–5</sup>

The pathophysiological correlates of those lesions are not fully understood yet. In SWI hypointense core lesions, severe demyelination or iron deposition as a consequence of dying iron-rich oligodendrocytes or blood brain barrier breakdown with haemoglobin leakage have been discussed as contributing to SWI signal loss.<sup>5,6</sup> Following this assumption, this lesion type rather reflects a relatively young than an old lesion.<sup>4,6–9</sup>

In SWI hypointense ring lesions, iron-rich active microglia were histopathologically observed that co-localise with the paramagnetic ring.<sup>10–15</sup> The 'ring sign' was thus suggested as an *in vivo* imaging feature of chronic active MS lesions that smoulder over time and may contribute to disability progression in progressive MS disease stages.<sup>10–15</sup>

If these hypotheses hold true, SWI signal changes may help to estimate the stage and chronic inflammatory activity of MS lesions, and potentially have diagnostic, therapeutic and prognostic implications.

Nevertheless, current studies have predominantly investigated lesion morphology and lesion evolution in patients with long-lasting MS, and little is known on the dynamics of SWI lesion morphology at the very beginning of the disease when neuroinflammation is believed to outweigh neurodegeneration.

Based on this background, we aimed to describe the presence of SWI hypointense core and ring lesions in patients with clinically isolated syndrome (CIS) and early MS. In addition, we asked whether SWI hypointense core lesions at this very early stage of the disease already develop into ring lesions, and whether the presence of such lesions at the beginning of the disease are associated with clinical or paraclinical worsening.

## Methods

### Study participants

Patients with CIS or relapsing–remitting MS as defined by the 2010 diagnostic panel criteria<sup>1</sup> were included from the Berlin CIS cohort. The Berlin cohort study of CIS and early MS (NCT01371071) is an observational, prospective study that follows patients over a period of at least 5 years to identify risk factors for relapses, prognostic factors and therapy response markers. Inclusion criteria are age

> 18 years, CIS within the last 6 months, and diagnosis of MS within the last two years. All patients with a SWI scan at baseline, and a follow-up of at least 18 months were eligible for this study. Magnetic resonance (MR) images of insufficient quality were excluded. Clinical disability was assessed by the Expanded Disability Status Scale (EDSS), the Symbol Digit Modalities Test (SDMT) as a marker of cognitive function, and the Multiple Sclerosis Functional Composite (MSFC) score including the Nine-Hole Peg Test (9HPT), the Timed 25-Foot Walk test (T25FWT) and the Paced Auditory Serial Addition Test (PASAT). The study was approved by the local ethics committee (EA1/182/10). Written informed consent was obtained from all participants before examination.

### MRI acquisition

MR images were acquired using a 3T Siemens whole body scanner (Trio TIM; Siemens, Erlangen, Germany). The imaging protocol included pre- and post-contrast three-dimensional T1\*w magnetization prepared rapid gradient echo (MPRAGE; spatial resolution =  $(1 \times 1 \times 1) \text{ mm}^3$ , gadolinium (0.1 mmol Gd/kg) was used as contrast agent), and a three-dimensional T2-weighted fluid-attenuated inversion recovery (T2w-FLAIR; spatial resolution =  $(1 \times 1 \times 1) \text{ mm}^3$ ). In addition, a three-dimensional gradient echo flow-compensated SWI (echo time = 28 ms, repetition time = 35 ms, flip angle =  $15^\circ$ , spatial resolution =  $(1 \times 1 \times 1) \text{ mm}^3$ ) yielding magnitude, filtered phase and reconstructed SWI images was acquired (see Supplemental Material for more details).

### Image analysis

MRI scans were analysed by NB, EB (medical students trained for the assessment of SWI lesion morphology) and TS (resident in neurology with experience in the analysis of gradient echo MR images such as SWI) in consensus reading, and blinded to clinical details. T2w-FLAIR hyperintense lesions with a diameter of > 3 mm were marked. Each T2w-FLAIR lesion was then looked up on co-registered SWI to describe the existence of a SWI hypointense core or a SWI hypointense ring at the edge of the lesion at baseline.

A hypointense core was defined as homogenous distributed SWI hypointense signal intensity within the centre of the lesion that is not related to a central vein as identified by its tubular appearance and pathway through the lesion edges. A hypointense ring was defined as SWI hypointense signal intensity at the edge of the lesion with rim-like appearance.

Lesions with irregular SWI hypointense signal without meeting the above criteria were characterised as lesions with diffuse SWI hypointense signal. Lesions without SWI hypointense signal were termed SWI isointense.

Contrast enhancement was assessed on post-contrast three-dimensional T1\*w MPRAGE images. Contrast-enhancing lesions with a SWI hypointense ring were classified as ‘acute ring lesions’, and non-contrast enhancing lesions with a SWI hypointense ring were classified as ‘chronic ring lesions’. Next, changes in lesion morphology were noted at follow-up.

We also assessed lesion volume (change), percentage of brain volume change (PBVC),<sup>16</sup> normalised mean intralesional T1w signal intensity, contrast enhancement, and the number of new lesions at follow-up (see Supplemental Material for more details).

### Statistical analysis

All analyses were performed using IBM SPSS Statistics (Version 20; IBM, Armonk, New York, USA). All  $p$  values  $< 0.05$  were considered significant. Because of the exploratory nature of the study, no adjustments for multiple comparisons were made. Most of the variables were not normally distributed. Thus, group differences were assessed by using a nonparametric Mann–Whitney U test (MWU), and we used Spearman correlation to test for associations between imaging and clinical variables. Dichotomous variables were compared by using Fisher’s exact test. Finally, we used general linear models (GLMs) with backward selection to assess the predictive value of SWI imaging markers ( $p$ -to-exclude = 0.1). Results were bootstrapped (resampling size  $n = 1000$ ) and confirmed by using Spearman correlation. PASAT, T25FWT and 9HPT scores were transformed into  $z$  scores. Relapse rates and PBVC were annualised.

## Results

### Study participants

Seventy-nine patients fulfilled the inclusion criteria, and 13 patients were subsequently excluded for technical reasons (insufficient SWI image quality, see also Supplemental Material Table 1 for missing values). Finally, 66 patients with CIS ( $n = 32$ ) or relapsing–remitting MS ( $n = 34$ ) were analysed and followed over a median period of 2.9 years (range 1.6–4.6 years). More demographic details are presented in Table 1.

### Lesion morphology at baseline

In total, we analysed 611 lesions at baseline. Of these, 64 lesions (10.5%, mean  $\pm$  standard deviation (SD) per patient, range,  $1.0 \pm 2.3$ , 0–12) had a SWI hypointense core, 28 lesions had a SWI hypointense ring (4.6%, mean  $\pm$  SD per patient, range,  $0.4 \pm 1.1$ , 0–6), and 19 lesions showed a diffuse SWI hypointense intralesional signal distribution (3.1%, mean  $\pm$  SD per patient, range,  $0.3 \pm 0.8$ , 0–5). The remaining 500 lesions (82%) were SWI isointense. Hypointense ring lesions without contrast enhancement were larger ( $p < 0.001$ ) and had lower normalised T1w intensity values ( $p < 0.001$ ) in comparison to lesions without a ring. The Supplemental Material provides more information including a description of the lesion morphology of gadolinium-enhancing lesions.

### The fate of SWI hypointense ring and core lesions

The ring sign persisted in 21 of all 28 ring lesions (75%, Figure 1). In seven lesions, the ring sign disappeared into SWI isointensity including all five lesions with contrast enhancement at baseline (‘acute ring sign’ lesions) as well as two others. Lesions with and without hypointense rings at baseline did not differ regarding change in normalised T1w intensity values (MWU,  $p = 0.207$ ) nor T2w-FLAIR lesion volume (MWU,  $p = 0.077$ ).

The hypointense core disappeared into SWI isointensity in 52 of 64 lesions (81%, Figure 2), nearly disappeared in two lesions (3%), and remained stable in eight lesions (13%).

During follow-up, a distinct ring sign developed out of two hypointense core (3%) and two diffuse hypointense lesions (Figure 3). Two of them showed contrast enhancement at baseline.

Lesions with and without a hypointense core at baseline did not differ regarding change in normalised T1w intensity values nor T2w-FLAIR lesion volume (all  $p < 0.290$ ). Nonetheless, more hypointense core lesions were classified as ‘shrinking’ in comparison to lesions without a hypointense core (Figure 4, Fisher’s exact test  $p = 0.002$ ).

### Group differences at baseline: MRI measures

Twenty patients (30%) had SWI hypointense core lesions. We did not observe statistical significant differences in age, gender, disease duration or treatment between patients with and without SWI hypointense core lesions (Table 1). Patients with SWI hypointense core lesions had more T2w-FLAIR

Molecular Medicine,  
Germany

**Klemens Ruprecht**,  
Department of Neurology,  
Charité-Universitätsmedizin  
Berlin, Germany

**Dominik Meier**,  
qbfg, Department of  
Biomedical Engineering,  
University of Basel,  
Switzerland  
Medical Image Analysis  
Center AG, Switzerland

**Jens Wuerfel\***,  
qbfg, Department of  
Biomedical Engineering,  
University of Basel,  
Switzerland  
Neurocure Clinical Research  
Center, Charité-  
Universitätsmedizin Berlin,  
Germany  
Medical Image Analysis  
Center AG, Switzerland

**Friedemann Paul\***,  
Neurocure Clinical Research  
Center, Charité-  
Universitätsmedizin Berlin,  
Germany  
Experimental and Clinical  
Research Center, Charité –  
Universitätsmedizin Berlin,  
and Berlin Institute of Health  
and Max Delbrück Center for  
Molecular Medicine,  
Germany  
Department of Neurology,  
Charité-Universitätsmedizin  
Berlin, Germany

**Tim Sinnecker\***,  
qbfg, Department of  
Biomedical Engineering,  
University of Basel,  
Switzerland  
Neurocure Clinical Research  
Center, Charité-  
Universitätsmedizin Berlin,  
Germany  
Medical Image Analysis  
Center AG, Switzerland  
Neurologic Clinic and  
Policlinic, Departments of  
Medicine, Clinical Research  
and Biomedical Engineering,  
University Hospital and  
University of Basel,  
Switzerland

**Table 1.** Cohort overview and comparison between subgroups.

	All patients	‘Ring sign’		‘Core sign’	
		Yes	No	Yes	No
Demographic data					
n	66	13	53	28	38
Female (n)	40	7	33, p = 0.753	16	24, p = 0.799
Age (years), mean ± SD, range	34 ± 8.6, 20–52	34.9 ± 9.8, 24–51	33.8 ± 8.4, 20–52, p = 0.921	35 ± 8, 23–51	33.4 ± 9, 20–52, p = 0.375
Disease duration (months), mean ± SD, range	17.9 ± 15.3, 0–52	23 ± 16.4, 0–38	16.7 ± 15, 0–52, p = 0.191	20.6 ± 16.1, 0–49	15.9 ± 14.7, 1–52, p = 0.380
Clinical and MRI findings at baseline					
EDSS, median, range	1.5, 0–4.5	2, 0–3	1.5, 0–4.5, p = 0.309	1.5, 0–3	1.5, 0–4.5, p = 0.686
Total lesion count (n), median, range	5, 0–45	18, 2–43	5, 0–45, p < 0.001	12, 3–45	3, 0–17, p < 0.001
Total lesion volume (mm <sup>3</sup> ), median, range	330, 0–8626	2002, 268–7647	218, 0–8626, p < 0.001	1464, 100–8626	113, 0–2168, p < 0.001
Additional clinical measures at baseline					
SDMT, median, range	61, 0–102	52, 0–68	64, 34–102, p = 0.031	60, 0–102	62, 34–86, p = 0.671
9HPT, median, range	18, 14–53	18, 15–53	18, 14–25, p = 0.409	18, 14–53	18, 15–25, p = 0.529
T25FWT, median, range	4, 3–9	4, 3–5	4, 3–9, p = 0.419	4, 3–5	4, 3–9, p = 0.822
PASAT, median, range	54, 0–60	57, 44–60	54, 0–60, p = 0.136	57, 0–60	53, 19–60, p = 0.091
Clinical and MRI findings at follow-up					
Number of new lesions (n), median, range	0, 0–17	0, 0–5	0, 0–17, p = 0.885	0, 0–10	0, 0–17, p = 0.750
Annualised PBVC (%), mean ± SD, range	−0.24 ± 0.47, −2.33–0.43	−0.33 ± 0.51, −1.36–0.39	−0.22 ± 0.46, −2.33–0.43, p = 0.453	−0.38 ± 0.43, −1.36–0.32	−0.14 ± 0.48, −2.33–0.43, p = 0.008
Annualised relapse rate, median, range	0, 0–1.8	0, 0–0.7	0, 0–1.8, p = 0.201	0, 0–1.8	0, 0–0.6, p = 0.851
EDSS, median, range	1.5, 0–5.5	2.5, 0–5.5	1, 0–5.5, p = 0.010	1.5, 0–5.5	1, 0–5.5, p = 0.094
Treatment					
Treatment at baseline (n, %)	No DMT: 36 (55%) Platform: 23 (35%) Oral: 7 (11%) Infusion: 0	No DMT: 5 (38%) Platform: 6 (46%) Oral: 2 (15%) Infusion: 0	No DMT: 31 (59%) Platform: 17 (32%) Oral: 5 (9%) Infusion: 0	No DMT: 10 (36%) Platform: 14 (50%) Oral: 4 (14%) Infusion: 0	No DMT: 26 (68%) Platform: 9 (23%) Oral: 3 (8%) Infusion: 0
Treatment at follow- up (n, %)	Unchanged: 44 (67%) Switch to plat- form: 6 (9%) Switch to oral: 10 (15%) Switch to infu- sion: 6 (9%)	Unchanged: 8 (62%) Switch to plat- form: 0 Switch to oral: 4 (31%) Switch to infu- sion: 1 (8%)	Unchanged: 36 (68%) Switch to plat- form: 6 (11%) Switch to oral: 6 (11%) Switch to infu- sion: 5 (9%)	Unchanged: 18 (64%) Switch to plat- form: 1 (4%) Switch to oral: 4 (14%) Switch to infu- sion: 5 (18%)	Unchanged: 26 (68%) Switch to plat- form: 5 (13%) Switch to oral: 6 (16%) Switch to infu- sion: 1 (3%)

9HPT: Nine-Hole Peg Test; EDSS: Expanded Disability Status Scale; MRI: magnetic resonance imaging; PASAT: Paced Auditory Serial Addition Test; PBVC: percentage of brain volume change; SD: standard deviation; SDMT: Symbol Digit Modalities Test; T25FWT: Timed 25-Foot Walk test.

Values of p are related to a comparison between patients with and without ‘ring sign’ or ‘core sign’ lesions. Platform: treatment with glatiramer acetate or beta-interferons. Oral: treatment with fingolimod, teriflunomide or dimethyl fumarate. Infusion: treatment with natalizumab or alemtuzumab.

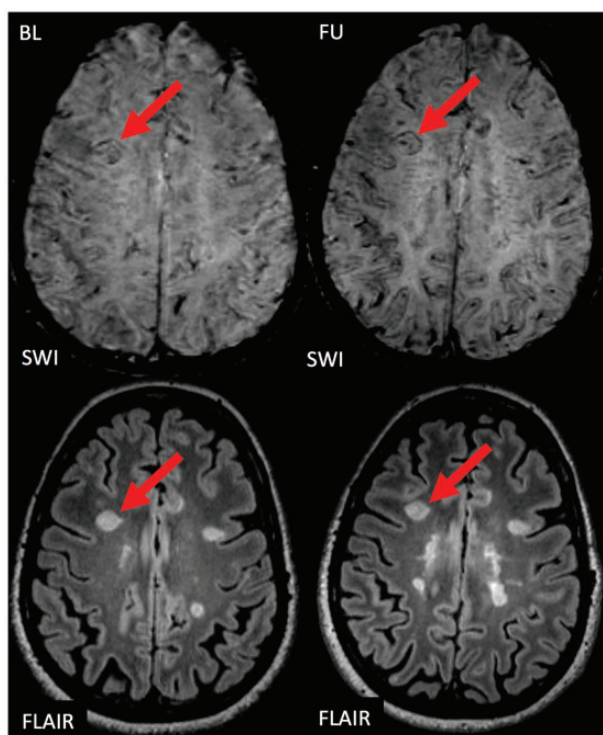


**Figure 1.** The fate of an exemplary ‘ring sign’ lesion.

Susceptibility weighted imaging (SWI; top) and T2 weighted fluid attenuated inversion recovery (T2w-FLAIR; bottom) images are shown at baseline (left) and follow-up (right). At baseline, a prominent hyperintense white matter lesion is visualised on T2w-FLAIR. The lesion is characterised by a SWI hypointense signal at the edge of the lesion (‘ring sign’). During follow-up, the appearance of the lesion on SWI and T2w-FLAIR does not change significantly. The ‘ring sign’ is still clearly visible, and the size of the lesion has not clearly changed. BL: baseline; FU: follow-up.

lesions (MWU,  $p < 0.001$ , Table 1), higher lesion volumes (MWU,  $p < 0.001$ , Table 1) and more contrast-enhancing lesions (MWU,  $p = 0.022$ ) at baseline.

Thirteen patients (19%) had SWI hypointense ring lesions. We did not observe significant differences in age, gender, disease duration or treatment between patients with and without SWI hypointense ring lesions (Table 1). Patients with SWI hypointense ring lesions had more T2w-FLAIR lesions (MWU,  $p < 0.001$ ), higher lesion volumes (MWU,  $p < 0.001$ ), more contrast enhancing lesions (MWU,  $p = 0.002$ ) and overall lower normalised intralésional T1w signal intensity values (MWU,  $p = 0.014$ ) at baseline (see Supplemental Material for more details).

#### *Group differences at baseline: clinical parameters*

Patients with SWI hypointense core or ring lesions, did not differ regarding clinical measures including sex, age, disease duration, EDSS, MSFC, 9HPT, T25FWT and PASAT (all  $p > 0.091$ , Table 1) except for patients with SWI hypointense ring lesions

who had lower SDMT values (MWU,  $p = 0.031$ , see Supplemental Material for more details).

#### *Predictive value of SWI markers at baseline:*

##### *MRI measures*

A higher number of SWI hypointense core lesions per patient at baseline correlated with higher rates of brain volume loss during follow-up (PBVC, Spearman,  $p < 0.001$ ,  $\rho = -0.424$ ), but did not predict the number of new lesions or the degree of mean normalised T1w signal intensity at follow-up (all  $p > 0.924$ , Table 1, see Supplemental Material for more details).

The number of SWI hypointense ring lesions at baseline did not predict the degree of brain atrophy during follow-up, the number of new lesions or the degree of mean normalised T1w signal intensity at follow-up (all  $p > 0.126$ , Table 1, see Supplemental Material for more details).

The analysis of the proportion of lesions with a SWI hypointense core or ring instead of the number of

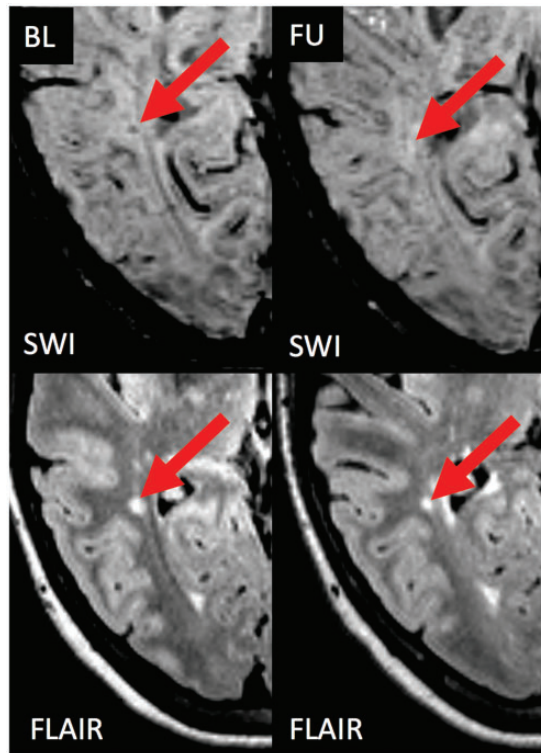


**Figure 2.** The fate of an exemplary ‘core sign’ lesion without contrast enhancement. Susceptibility weighted imaging (SWI; top) and T2 weighted fluid attenuated inversion recovery (T2w-FLAIR; bottom) images are shown at baseline (left) and follow-up (right). At baseline, a hyperintense white matter lesion is visualised on T2w-FLAIR. The lesion is characterised by a SWI hypointense signal within the centre of the lesion (‘core sign’). During follow-up, the lesion became smaller on T2w-FLAIR, and the SWI hypointense signal (‘core sign’) disappeared rendering the lesion isointense to slightly hyperintense on SWI. BL: baseline; FU: follow-up.

lesions did not significantly change the results (data not presented).

#### *Predictive value of SWI markers at baseline: clinical parameters*

An EDSS increase was observed in 17 patients (26%). Patients with SWI hypointense ring lesions had higher EDSS values at follow-up (MWU,  $p=0.010$ , Table 1) and showed a higher EDSS increase (MWU,  $p=0.032$ , Figure 5). In addition, the number of SWI hypointense ring lesions per patient correlated with higher EDSS values at follow-up (Spearman,  $p=0.005$ ,  $\rho=0.342$ ), and EDSS change (Spearman,  $p=0.021$ ,  $\rho=0.289$ ). By using a general linear model with backward selection and EDSS at follow-up as the dependent variable, and sex, age, disease duration, disease

course, EDSS at baseline, lesion count, lesion volume, number of contrast enhancing lesions and SWI hypointense ring/core lesions as independent variables, only age ( $B=0.029$ ,  $p=0.042$ ), EDSS at baseline ( $B=0.723$ ,  $p<0.001$ ) and the number of SWI hypointense ring lesions at baseline ( $B=0.371$ ,  $p=0.001$ ) remained significant within the model ( $R^2=0.587$ ,  $p<0.001$ ) and thus were predictive for the EDSS at follow-up (see Supplemental Material for more analyses that better illustrate that this association is independent of the overall T2w-FLAIR lesion load). The results were confirmed by bootstrapping.

We did not observe an association between the number of SWI hypointense core or ring lesions and any other clinical measures at follow-up including EDSS (hypointense core lesions), number of relapses, conversion from CIS to RRMS, MSFC, 9HPT, T25FWT, PASAT and SDMT (all  $p>0.250$ ). Accordingly, patients with SWI hypointense core lesions and patients with SWI hypointense ring lesions did not differ from patients without such lesions regarding these clinical outcome measures (all  $p>0.094$ , Table 1).

The analysis of the proportion of lesions with a SWI hypointense core or ring instead of the number of lesions did not significantly change the results (data not presented).

#### **Discussion**

In this study we have investigated the temporal evolution of SWI hypointense ring and core lesions in a rather young early MS and CIS cohort to assess the prognostic relevance of these novel MRI biomarkers at the very beginning of the disease.

We observed that only a relatively small proportion of patients within our cohort had hypointense ring lesions while more patients had hypointense core lesions. Patients with either hypointense ring or core lesions had more T2w-FLAIR lesions at baseline. During follow-up, the majority of hypointense core lesions became SWI isointense and/or shrunk. Few hypointense core lesions developed into hypointense ring lesions. Hypointense ring lesions did not shrink, and only sporadic become SWI isointense over time. Finally, patients with SWI hypointense ring lesions at baseline had a more severe EDSS progression than patients without.

SWI is a gradient echo imaging technique that is sensitive to changes of the magnetic field on the

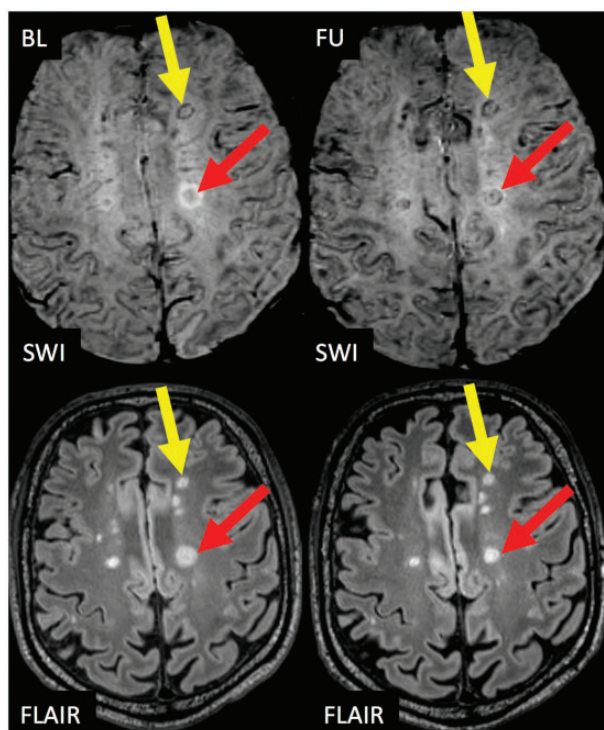


**Figure 3.** Transition of a ‘core sign’ lesion into a ‘ring sign’ lesion.

Susceptibility weighted imaging (SWI; top) and T2 weighted fluid attenuated inversion recovery (T2w-FLAIR; bottom) images are shown at baseline (left) and follow-up (right). At baseline, a prominent hyperintense white matter lesion is visualised on T2w-FLAIR (red arrow). The lesion is characterised by a SWI hypointense signal within the centre of the lesion (‘core sign’). During follow-up, the appearance of the lesion on SWI changes. The ‘core sign’ is not visible anymore, but a distinct SWI hypointense ring (‘ring sign’) has been formed. Also, a vein is now visible within the centre of the lesion (‘central vein sign’ indicated by the black dot within the lesion centre as the vein runs perpendicular to the image plane) that was previously ‘covered’ by the ‘core sign’. Also note the ‘ring sign’ lesion that is already visible at baseline (yellow arrow), which did not change its size or morphology during follow-up (yellow arrow). BL: baseline; FU: follow-up.

microscopic level.<sup>11,17</sup> Thus, the presence of paramagnetic substances and changes in the magnetic microstructure of the tissue will lead to signal changes on SWI.<sup>17</sup> This makes SWI – and other gradient echo MR imaging techniques such as T2\*w imaging and quantitative susceptibility mapping (QSM) – an attractive imaging technique to explore new imaging biomarkers as it provides additional information on top of conventional MR measures.

In MS, different imaging patterns were described on SWI.<sup>18,19</sup> In a varying proportion of MS lesions, a distinct SWI hypointense core can be visualised.<sup>3,5,20,21</sup> The pathophysiological correlate of this imaging finding is not fully understood, but our data show that the SWI hypointense core does not resemble T1w hypointense lesions. One hypothesis is that the SWI hypointense core is either the consequence of a loss of diamagnetic myelin

because of severe demyelination or paramagnetic iron deposits.<sup>5,20,22</sup> But where does the iron come from? Oligodendrocytes are by far the predominant iron-containing cells in the brain as they carry iron-requiring enzymes necessary for myelin production.<sup>23</sup> Intra-lesional iron deposits may thus be the consequence of dying oligodendrocytes releasing iron into the extracellular space, or reflect an increased iron-demand of oligodendrocytes during re-myelination.<sup>23–25</sup> Another idea is that intra-lesional iron deposits derive from leaky blood vessels within the MS lesions as a consequence of blood brain barrier (BBB) breakdown.<sup>20,22</sup> The observation that many young MS lesions with a nodular contrast enhancement as a sign of BBB breakdown are QSM negative, however, argues against this hypothesis.<sup>9,26,27</sup> In any case, all these assumptions suggest that a SWI hypointense core is a sign of disease activity and/or subsequent early repair mechanisms and thus probably reflect an imaging feature of

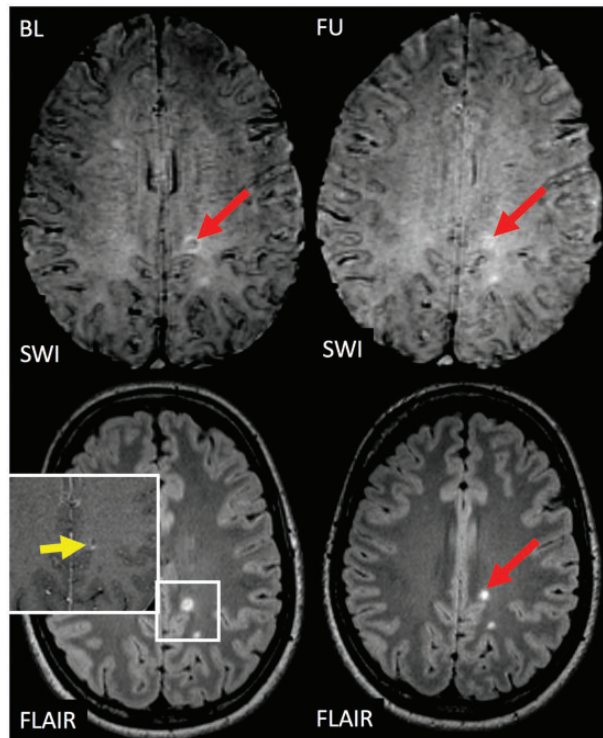


**Figure 4.** The fate of an exemplary contrast enhancing ‘core sign’ lesion. The figure illustrates susceptibility weighted imaging (SWI; top) and T2 weighted fluid attenuated inversion recovery (T2w-FLAIR; bottom) images at baseline (left) and follow-up (right). At baseline, a subcortical hyperintense white matter lesion is visualised on T2w-FLAIR. The lesion shows contrast enhancement (yellow arrow) and exhibits a SWI hypointense signal within the centre of the lesion (‘core sign’). During follow-up, the lesion became smaller on T2w-FLAIR, and the SWI hypointense signal (‘core sign’) disappeared rendering the lesion slightly hyperintense on SWI. BL: baseline; FU: follow-up.

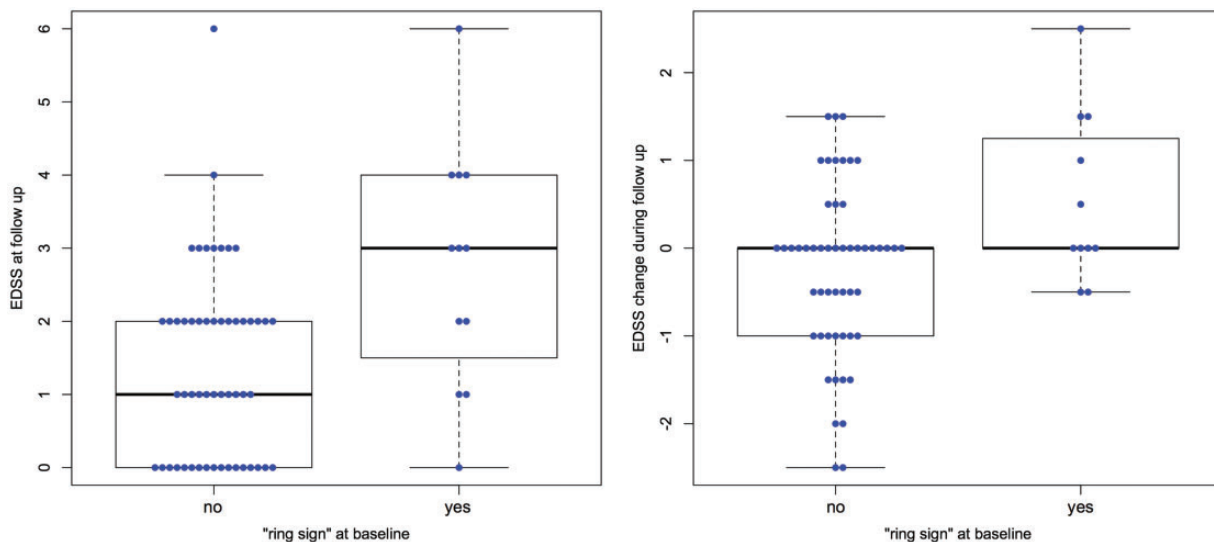


**Figure 5.** Boxplots. Boxplots on group differences in Expanded Disability Status Scale (EDSS) at follow-up (left) and EDSS change (right) between patients with and without ‘ring sign’ lesions at baseline are displayed. Patients with ‘ring sign’ lesions at baseline had higher EDSS values at follow-up (left,  $p=0.010$ ) and showed a higher change in EDSS (right,  $p=0.032$ ).



rather younger than older MS lesions.<sup>6,7</sup> Our results strongly support this hypothesis as a relevant proportion of SWI hypointense core lesions shrunk or became SWI isointense over time. Also, a decrease in magnetic susceptibility over time was described in MS lesions<sup>7</sup> and paramagnetic MR signal changes were more often observed in MS patients with a short versus long disease duration.<sup>6</sup> Both observations are in good agreement with our results. The ‘young lesion hypothesis’ of SWI hypointense core lesions may also explain the association between the latter and higher T2w-FLAIR lesion counts or increased rates of future brain atrophy as a consequence of Wallerian degeneration. Please note that the statistical analysis remained inconclusive whether brain atrophy was indeed predicted by SWI hypointense core lesions as SWI hypointense core lesions and T2w-FLAIR lesion counts were intercorrelated.

In addition, acute and chronic paramagnetic or SWI hypointense rings (‘ring sign’) were described around a proportion of MS lesions.<sup>10–15</sup> Acute rings are rather thin and typically co-localise with the area of contrast enhancement in ring enhancing MS lesions.<sup>28</sup> They are likely to reflect spreading inflammatory activity including higher concentrations of proteins at the lesion edges, rather than iron deposition.<sup>28</sup> Our data is well in line with this hypothesis as most SWI hypointense rings around contrast enhancing lesions disappeared over time suggesting that this is a rather transient feature of acute MS lesions. In contrast, chronic rings are more prominent or thick on gradient echo images<sup>28</sup> and were shown to persist over a longer period of time.<sup>4,12,29</sup> Histopathological and PET data suggest that the SWI hypointense ring corresponds to iron within CD68 positive cells such as microglia or macrophages at the edge of (chronic) active MS lesions.<sup>10–15</sup> One hypothesis is that microglia and/or macrophages incorporate and redistribute the iron from the centre of the lesion to the edge during lesion development as iron sequestration by macrophages is an important inflammatory response.<sup>30</sup> This idea is further supported by a recent experimental study showing that iron induces M1 polarization of macrophages and that iron uptake is regulated by proinflammatory cytokines.<sup>30</sup> Our data is well in line with this hypothesis as we - for the best of our knowledge - for the first time visualised the development of a SWI hypointense ring out of a SWI hypointense core lesion *in vivo*, which might indicate a redistribution of iron as discussed above.

Following the idea of the ‘ring sign’ as an *in vivo* biomarker of chronic active MS lesions, different research groups have investigated whether the ‘ring sign’ is a feature of smoldering or slowly enlarging lesions and whether the presence of ‘ring sign’ lesions is associated with a worse clinical outcome.<sup>6,12,16–19,31–35</sup> While some studies have indeed described an association of the ‘ring sign’ with progressive MS,<sup>33</sup> higher levels of clinical disability<sup>17,33</sup> and smoldering lesions,<sup>12,31</sup> others did not observe such relationships.<sup>6,16,32,34,35</sup> These discrepancies are likely to be the consequence of different study populations, sample sizes and follow-up intervals. A long follow-up is of high relevance, as the lesions grow with a rate of less than 1 mm per year.<sup>12</sup> Our data, which includes a follow-up of up to 4.6 years did not show an enlargement of ‘ring sign’ lesions over time, but in contrast to ‘core sign’ lesions, ‘ring sign’ lesions did not shrink and showed a trend towards more enlargement compared to other lesions. Hence, it remains inconclusive whether the ‘ring sign’ is indeed a marker of slowly enlarging lesions.

Nevertheless, the existence of ‘ring sign’ lesions at baseline was associated with the degree of disability as measured by EDSS and SDMT as well as disability worsening at follow-up as measured by (change in) EDSS. This supports the idea that patients with ‘ring sign’ lesions are somehow characterised by a proinflammatory stage.<sup>12,13,31</sup> The magnitude of this association was, however, only moderate, and we did not observe an association with additional markers of disease progression, which suggest that other (unknown) factors significantly contribute to disability progression in CIS and early MS.

Our study is not free of limitations. Although we followed all participants over a median period of 2.9 years, this follow-up could still be too short in order to detect relatively small volume changes within slowly expanding lesions. A much longer follow-up interval is probably needed to fully understand the evolution of ring lesions in terms of size and SWI signal intensity. Also, study participants were treated with a mix of different disease modifying therapies. Although we did not observe clear differences in lesion morphology between treatment groups, the number of study participants within subgroups was limited, and the potential treatment effect of disease modifying therapies on the development of ring sign lesions remains largely unknown. Finally, the overall degree of disease activity was relatively low in this cohort, which

may have reduced the power in detecting associations between SWI image characteristics and clinical outcome measures including cognitive function.

In conclusion, hypointense core lesions were frequently detectable in patients with CIS or early MS and are likely to reflect early MS lesion stages as most of them become SWI isointense over time. In our CIS and early MS cohort, only few hypointense core developed into hypointense ring lesions, and hypointense ring lesions were only rarely detectable at all. If present, they were associated with future disability progression, which renders them interesting for future clinical trials and personalised health directed approaches.

### Conflict of Interests

The author(s) declared no potential conflicts of interest with respect to the research, authorship, and/or publication of this article: NB, EB, SA, NS, LR, MS and AB do not report a potential conflict of interest. JBS has received travel grants and speaking fees from Bayer Healthcare, Biogen Idec, Merck Serono, Sanofi Genzyme, Teva Pharmaceuticals, and Novartis. KR was supported by the German Ministry of Education and Research (BMBF/KKNMS, Competence Network Multiple Sclerosis) and has received research support from Novartis and Merck Serono as well as speaking fees and travel grants from Guthy Jackson Charitable Foundation, Bayer Healthcare, Biogen Idec, Merck Serono, Sanofi-Aventis/Genzyme, Teva Pharmaceuticals, Roche and Novartis. DM is an employee of the Medical Image Analysis Center AG in Basel. JW is an employee of MIAC AG Basel, Switzerland. He served on scientific advisory boards of Actelion, Biogen, Genzyme-Sanofi, Novartis, and Roche. He is or was supported by grants of the EU (Horizon2020), BMBF and of Economic Affairs and Energy (BMWi). FP serves on the scientific advisory board for Novartis; received speaker honoraria and travel funding from Bayer, Novartis, Biogen Idec, Teva, Sanofi-Aventis/Genzyme, Merck Serono, Alexion, Chugai, MedImmune and Shire; is an academic editor for PLoS One; is an associate editor for Neurology Neuroimmunology and Neuroinflammation; consulted for SanofiGenzyme, Biogen Idec, MedImmune, Shire and Alexion; and received research support from Bayer, Novartis, Biogen Idec, Teva, Sanofi-Aventis/Genzyme, Alexion, Merck Serono, German Research Council, Werth Stiftung of the City of Cologne, BMBF, Arthur Arnstein Stiftung Berlin, EU FP7 Framework Program, Arthur Arnstein Foundation Berlin, Guthy Jackson Charitable Foundation and National Multiple Sclerosis Society of the USA.

TS has received travel support from Actelion and Roche, and speaker fees from Biogen. He is an employee of the MIAC AG Basel, Switzerland.

### Funding

The author(s) disclosed receipt of the following financial support for the research, authorship, and/or publication of this article: This study was supported by the German Research Council (DFG EXC 257).

### ORCID iDs

Eveline Brunner  <https://orcid.org/0000-0002-4617-2989>

Susanna Asseyer  <https://orcid.org/0000-0001-6289-1791>

Alexander Brandt  <https://orcid.org/0000-0002-9768-014X>

### Supplemental Material

Supplemental material for this article is available online.

### References

1. Polman CH, Reingold SC, Banwell B, et al. Diagnostic criteria for multiple sclerosis: 2010 Revisions to the McDonald criteria. *Ann Neurol* 2011; 69: 292–302.
2. Filippi M, Preziosa P, Banwell BL, et al. Assessment of lesions on magnetic resonance imaging in multiple sclerosis: Practical guidelines. *Brain J Neurol* 2019; 142: 1858–1875.
3. Sinnecker T, Schumacher S, Mueller K, et al. MRI phase changes in multiple sclerosis vs neuromyelitis optica lesions at 7T. *Neurol Neuroimmunol Neuroinflammation* 2016; 3: e259.
4. Chawla S, Kister I, Sinnecker T, et al. Longitudinal study of multiple sclerosis lesions using ultra-high field (7T) multiparametric MR imaging. *PLoS One* 2018; 13: e0202918.
5. Chawla S, Kister I, Wuerfel J, et al. Iron and non-iron-related characteristics of multiple sclerosis and neuromyelitis optica lesions at 7T MRI. *AJNR Am J Neuroradiol* 2016; 37: 1223–1230.
6. Bozin I, Ge Y, Kuchling J, et al. Magnetic resonance phase alterations in multiple sclerosis patients with short and long disease duration. *PLoS One* 2015; 10: e0128386.
7. Chen W, Gauthier SA, Gupta A, et al. Quantitative susceptibility mapping of multiple sclerosis lesions at various ages. *Radiology* 2014; 271: 183–192.
8. Zivadinov R, Dwyer M, Markovic-Plese S, et al. A pilot, longitudinal, 24-week study to evaluate the effect of interferon beta-1a subcutaneous on changes in susceptibility-weighted imaging-filtered phase assessment of lesions and subcortical deep-gray matter in relapsing–remitting multiple sclerosis. *Ther Adv Neurol Disord* 2015; 8: 59–70.
9. Zhang Y, Gauthier SA, Gupta A, et al. Longitudinal change in magnetic susceptibility of new enhanced multiple sclerosis (MS) lesions measured on serial quantitative susceptibility mapping (QSM). *J Magn Reson Imaging* 2016; 44: 426–432.

10. Pitt D, Boster A, Pei W, et al. Imaging cortical lesions in multiple sclerosis with ultra-high-field magnetic resonance imaging. *Arch Neurol* 2010; 67: 812–818.
11. Wiggermann V, Hametner S, Hernández-Torres E, et al. Susceptibility-sensitive MRI of multiple sclerosis lesions and the impact of normal-appearing white matter changes. *NMR Biomed* 2017; 30: e3727.
12. Dal-Bianco A, Grabner G, Kronnerwetter C, et al. Slow expansion of multiple sclerosis iron rim lesions: Pathology and 7 T magnetic resonance imaging. *Acta Neuropathol (Berl)* 2017; 133: 25–42.
13. Gillen KM, Mubarak M, Nguyen TD, et al. Significance and in vivo detection of iron-laden microglia in white matter multiple sclerosis lesions. *Front Immunol* 2018; 9: 255.
14. Popescu BF, Frischer JM, Webb SM, et al. Pathogenic implications of distinct patterns of iron and zinc in chronic MS lesions. *Acta Neuropathol* 2017; 134: 45–64.
15. Kaunzner UW, Kang Y, Zhang S, et al. Quantitative susceptibility mapping identifies inflammation in a subset of chronic multiple sclerosis lesions. *Brain J Neurol* 2019; 142: 133–145.
16. Smith SM, Zhang Y, Jenkinson M, et al. Accurate, robust, and automated longitudinal and cross-sectional brain change analysis. *Neuroimage* 2002; 17: 479–489.
17. Sukstanskii AL and Yablonskiy DA. On the role of neuronal magnetic susceptibility and structure symmetry on gradient echo MR signal formation. *Magn Reson Med* 2014; 71: 345–353.
18. Cronin MJ, Wharton S, Al-Radaideh A, et al. A comparison of phase imaging and quantitative susceptibility mapping in the imaging of multiple sclerosis lesions at ultrahigh field. *MAGMA* 2016; 29: 543–557.
19. Castellaro M, Magliozzi R, Palombit A, et al. Heterogeneity of cortical lesion susceptibility mapping in multiple sclerosis. *Am J Neuroradiol* 2017; 38: 1087–1095.
20. Bagnato F, Hametner S, Yao B, et al. Tracking iron in multiple sclerosis: A combined imaging and histopathological study at 7 Tesla. *Brain J Neurol* 2011; 134: 3602–3615.
21. Yao B, Bagnato F, Matsuura E, et al. Chronic multiple sclerosis lesions: Characterization with high-field-strength MR imaging. *Radiology* 2012; 262: 206–215.
22. Adams CW. Perivascular iron deposition and other vascular damage in multiple sclerosis. *J Neurol Neurosurg Psychiatry* 1988; 51: 260–265.
23. Connor JR and Menzies SL. Relationship of iron to oligodendrocytes and myelination. *Glia* 1996; 17: 83–93.
24. Hametner S, Wimmer I, Haider L, et al. Iron and neurodegeneration in the multiple sclerosis brain. *Ann Neurol* 2013; 74: 848–861.
25. Stephenson E, Nathoo N, Mahjoub Y, et al. Iron in multiple sclerosis: Roles in neurodegeneration and repair. *Nat Rev Neurol* 2014; 10: 459–468.
26. Zhang Y, Gauthier SA, Gupta A, et al. Magnetic susceptibility from quantitative susceptibility mapping (QSM) can differentiate new enhancing from non-enhancing multiple sclerosis lesions without gadolinium injection. *AJNR Am J Neuroradiol* 2016; 37: 1794–1799.
27. Zhang Y, Gauthier SA, Gupta A, et al. Quantitative susceptibility mapping and R2\* measured changes during white matter lesion development in multiple sclerosis: Myelin breakdown, myelin debris degradation and removal, and iron accumulation. *AJNR Am J Neuroradiol* 2016; 37: 1629–1635.
28. Absinta M, Sati P, Gaitán MI, et al. Seven-tesla phase imaging of acute multiple sclerosis lesions: A new window into the inflammatory process. *Ann Neurol* 2013; 74: 669–678.
29. Bian W, Harter K, Hammond-Rosenbluth KE, et al. A serial in vivo 7T magnetic resonance phase imaging study of white matter lesions in multiple sclerosis. *Mult Scler* 2013; 19: 69–75.
30. Mehta V, Pei W, Yang G, et al. Iron is a sensitive biomarker for inflammation in multiple sclerosis lesions. *PloS One* 2013; 8: e57573.
31. Absinta M, Sati P, Schindler M, et al. Persistent 7-tesla phase rim predicts poor outcome in new multiple sclerosis patient lesions. *J Clin Invest* 2016; 126: 2597–2609.
32. Hagemeyer J, Heininen-Brown M, Poloni GU, et al. Iron deposition in multiple sclerosis lesions measured by susceptibility-weighted imaging filtered phase: A case control study. *J Magn Reson Imaging* 2012; 36: 73–83.
33. Harrison DM, Li X, Liu H, et al. Lesion heterogeneity on high-field susceptibility MRI is associated with multiple sclerosis severity. *AJNR Am J Neuroradiol* 2016; 37: 1447–1453.
34. Yao B, Ikonomidou VN, Cantor FK, et al. Heterogeneity of multiple sclerosis white matter lesions detected with T2\*-weighted imaging at 7.0 Tesla. *J Neuroimaging* 2015; 25: 799–806.
35. Kuchling J, Ramien C, Bozin I, et al. Identical lesion morphology in primary progressive and relapsing-remitting MS—an ultrahigh field MRI study. *Mult Scler* 2014; 20: 1866–1871.